Chemical Engineering Science, 1977 Vol 32 pp 393–412 Pergamon Press Printed in Great Britain

CATALYST POISONING AND FIXED BED REACTOR DYNAMICS—II

ADIABATIC REACTORS

THOMAS H PRICE† and JOHN B BUTT‡
Department of Chemical Engineering and Ipatieff Catalytic Laboratory, Northwestern University, Evanston, IL 60201, U S A

(*Received* 15 *January* 1976, *accepted* 21 *May* 1976)

Abstract—Prior work on experimental and modeling studies of nonisothermal nonadiabatic reactor dynamics induced by catalyst poisoning is extended in this paper to adiabatic reactors Thiophene poisoning of the nickel catalyzed hydrogenation of benzene is used as the experimental system

A pseudohomogeneous one dimensional dispersion model was used to model both steady state and transient behavior of the reactor on introduction of poison into the feed Poisoning kinetics were interpreted via a shell-progressive mechanism which appears to provide a plausible and simpler alternative to the two site mechanism previously postulated[1] In general a reasonable agreement between experiment and model was obtained, however the accumulation of errors involved in separate determination of the reactor/reaction parameters ultimately limits the degree of precision which such simulations can attain

INTRODUCTION

We have recently reported an experimental and modeling study of fixed bed reactor dynamics due to catalyst poisoning in a non-adiabatic, non-isothermal system[1] Benzene hydrogenation on Ni-kieselguhr, poisoned by thiophene, was used as a model exothermic reaction A primary objective of the study was to determine how far one might go in *a priori* modeling of such dynamics, i e simulation in terms of reasonable reactor models for which all parameters involved are determined in independent experimentation The results of that study indicated partial but not total attainment of this objective, the major difficulties reported were centered around the interrelationship between the intrinsic kinetics of deactivation and the total adsorption capacity of the catalyst for poison The present work extends this investigation of reactor dynamics to adiabatic reactors, where the troublesome problem of wall heat transfer is absent and the specific effects of deactivation are more easily identifiable The same reaction system and general procedures reported previously[1] have been employed

REACTOR MODEL

A complete one-dimensional, pseudo-homogeneous dispersion model written to satisfy the experimental conditions of this study is

(1) Benzene mass balance

$$\frac{\partial x_B}{\partial t} = D_{eB}\frac{\partial^2 x_B}{\partial z^2} - U\frac{\partial x_B}{\partial z} - \frac{MW_g\ \rho_B}{\epsilon\rho_g}(r_B)\theta \qquad (1)$$

(2) Thiophene mass balance

$$\frac{\partial x_T}{\partial t} = D_{eT}\frac{\partial^2 x_T}{\partial z^2} - U\frac{\partial x_T}{\partial z} - \frac{MW_g\ \rho_B}{\epsilon\rho_g}(r_T)\theta \qquad (2)$$

(3) Energy balance

$$\frac{\partial T}{\partial t} = \frac{\lambda_e}{\langle\rho cp\rangle}\frac{\partial^2 T}{\partial z^2} - \frac{U\rho_g Cp_g}{\langle\rho cp\rangle}\frac{\partial T}{\partial z} + \frac{(-\Delta H)}{\langle\rho cp\rangle}\frac{\rho_g\epsilon}{MW_g}(r_B)\theta \qquad (3)$$

In eqns (1)–(3) θ is an activity variable taken to be separable from the intrinsic kinetic expressions, r_B and r_T, and is given by[1]

$$\frac{d\theta}{dt} = r_d = \frac{r_T}{M_T} = -k_d^0\, e^{-E_d/RT} P x_T \theta \qquad (4)$$

The hydrogenation kinetics are[2]

$$r_B = \frac{k^0 K^0 \exp[(-Q-E)/RT]P^2 x_B x_H}{1 + K^0 \exp(-Q/RT) P x_B} \qquad (5)$$

The boundary conditions employed in the simulation correspond to the physical configuration of the reactor, with inert fore and aft packed sections surrounding the active bed

$$T(z=0) = T_0, \frac{\partial T}{\partial z}(z=L) = 0$$

$$x_i(z=Z1) = x_{i_0}, \frac{\partial x_i}{\partial z}(Z=z2) = 0 \qquad (6)$$

The major assumptions involved in the above model equations, aside from that of pseudo-homogeneity, are omission of the hydrogen mass balance, use of a linear poisoning kinetics model, separability[3] of deactivation

†Current address Stauffer Chemical Company Richmond, CA 94802, U S A
‡To whom correspondance should be addressed

rates from the major reaction rate, and neglect of interphase and intraparticle gradients The large excess of hydrogen employed in all experiments provides justification for the first of these, specifics of the other assumptions will be discussed subsequently

EXPERIMENTAL

The general experimental procedures, conditions, reagents, and apparatus were the same as those reported by Weng *et al* [1] The reactor flow system employs a parallel feed arrangement, one containing a pure benzene-hydrogen mixture and the second a thiophene - benzene - hydrogen mixture In operation, the pure feed is initially passed through the reactor, establishing a steady state, while the contaminated feed at identical conditions of temperature and flow rate passes through a dummy reactor Once steady state is achieved with the first stream a four way valve is switched, sending the second stream through the active reactor and the first through the dummy Primary experimental data consist of axial temperature profiles along the reactor and inlet and exit compositions of all components as a function of time of operation

Adiabatic operation in small scale laboratory reactors is notoriously difficult to achieve In this work a concentric double tubing, condenser-like glass reactor, shown in Fig 1, was employed To ensure adiabatic operation, the jacket was evacuated to $\sim 10^{-8}$ torr, the inner jacket walls silvered to minimize radiation effects, and the entire reactor assembly enclosed in contoured asbestos brick

The primary series of experiments encompassed a range of temperatures from 50–190°C, total pressure of one atm, inlet benzene concentrations of ~1 5 mole%, and inlet thiophene concentrations from 0 03 to 0 065 mole% A summary of experimental conditions is given in Table 1 In these runs generally only one experimental variable was changed at a time Taking A5 as a base condition, the following pertain

A4 50% lower inlet thiophene concentration

A6 30% lower inlet flow rate

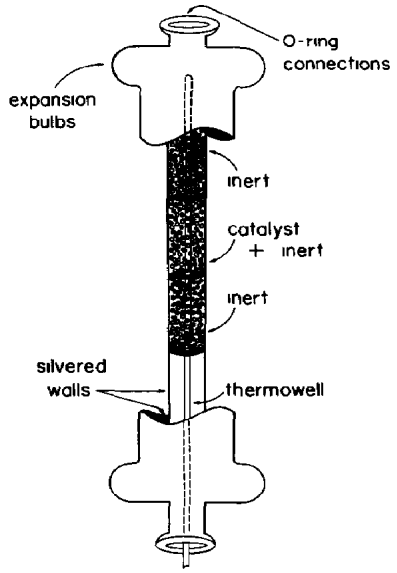

Fig 1 Pictorial view of the experimental reactor

A7 as A6, but with 3 times catalyst density and twice as much total catalyst

A8 60/70 mesh catalyst particle size

Typical experimental temperature profiles are shown for Run A5 in Fig 2 It is seen that there is some fall-off in temperature downstream of the reaction zone, this was encountered to some extent in all experiments, so that in spite of our best efforts we must grudgingly admit that the reactor is only "nearly-adiabatic" The active zone in the bed, however, is adiabatic and heat losses are important only in modeling temperature profiles in the aft-section of the reactor, i e after everything has happened Corresponding exit concentrations of benzene and thiophene for A5 are given in Fig 3

INTERPRETATION

Parameters and assumptions

There are 17 parameters involved in the description of

Table 1 Operating conditions—adiabatic runs

Run	Flow (m^3/sec) (10^5)	x_B (10^2)	x_T (10^4)	P (N/m^2) (10^{-5})	T_s (°C)	T_o (°C)	ρ_B (kg/m^3) (10^{-2})	ρ_T (kg/m^3) (10^{-3})	Wt of Catalyst (kg)(10^3)	Entrance Length (m)	Catalyst Length (m)	Particle Mesh Size
A4	2 50	1 41	3 16	1 000	23 7	45 6	4 14	1 15	8 985	0 188	0 118	12/20
A5	2 45	1 42	6 36	1 010	23 0	49 0	4 16	1 16	8 987	0 184	0 116	12/20
A6	1 60	1 42	6 34	1 010	23 2	48 6	4 39	1 22	8 987	0 181	0 111	12/20
A7	1 58	1 45	6 48	1 000	24 8	46 2	13 53	13 53	17 978	0 174	0 072	12/20
A8	2 47	1 46	6 53	0 985	24 4	52 8	4 25	1 18	8 988	0 151	0 115	60/70
Example (Fig 5,11)	1 98	1 80	4 04	0 993	24 4	56 0	3 90	1 08	10 109	0 136	0 103	12/20

Reactor dimensions length = 0 4578 m, radius = 0 0078 m
thermowell = 0 03 m O D

Catalyst Harshaw Ni - 0104T, mesh sizes as indicated, diluted 2 1 with glass beads of same dimension

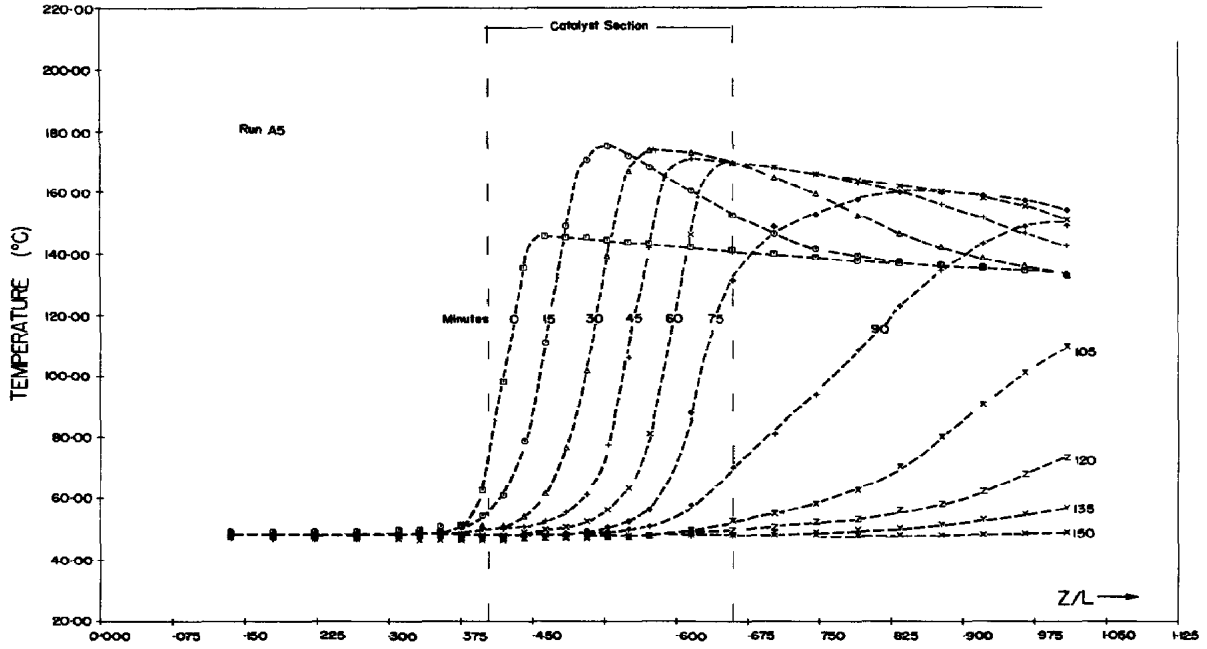

Fig 2 Typical measured temperature profiles, Run A5

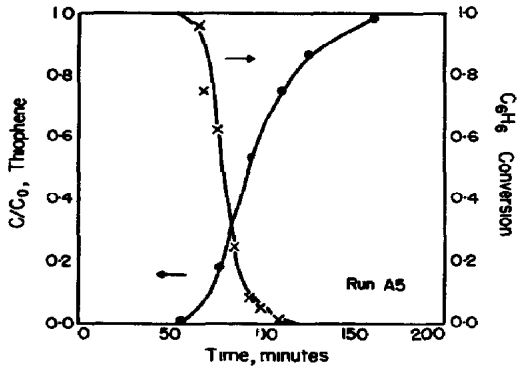

Fig 3 Time history of exit benzene and thiophene concentrations, Run A5

the experimental system afforded by eqns (1)–(5) In accordance with the philosophy of *a priori* modeling, these have all been determined either in independent experimentation or, when available, via reliable literature correlation A listing of the parameters and their values for these experiments is given in Table 2

Computational results demonstrate the very small effect of mass dispersion in this system[5] The correlation of Evans and Kenny[10] predicts $Pe_m \approx 5$ for the conditions of these experiments, corresponding to the molecular diffusivities given in Table 2 Thermal dispersion, however, is very important The steady state temperature profiles in the fore and aft sections of the reactor were matched via nonlinear regression to the analytical solution of the steady state energy balance to obtain values for λ_e After correcting for contributions due to wall conduction, effective bed conductivities agreed to within ±10% of the Yagi–Kunii[11] correlation The corresponding value of Pe_h is ≈0 2

The apparent thiophene capacity of the catalyst, M_T, was measured in each of the experiments via mass balance difference between inlet and exit concentrations of thiophene over the duration of a deactivation run These were found to vary according to experimental conditions, the reason for this is discussed subsequently Determination of the remaining parameters is relatively straightforward and is discussed in detail by Weng[9] and Price[5]

A central point in the model of eqns (1)–(5) is the assumption of negligible influence of interphase and intraparticle gradients In laboratory reactors, generally restricted to relatively low flow rates, interphase heat resistance is dominant over intraparticle resistance[12] Specifically, if $Bi_h < 5$, then intraparticle temperature gradients are negligible For the Reynolds Numbers of these experiments ($Re \approx 2$), the most reliable literature to date[13] predicts $Bi_h \approx 1$ Assuming that $j_D = j_H$, the corresponding $Bi_m \approx 6\,5$ Table 3 gives values of the various catalyst and fluid parameters pertinent to the analysis of transport gradients

For a less than 5% deviation in the rate due to interphase temperature gradients, Mears[14] requires that

$$\frac{(-\Delta H)(r_B)(r_p)}{hT} \leq \frac{0\,15}{\delta} \tag{7}$$

or, for these experiments

$$0\,3 \leq 0\,05$$

The order of magnitude violation of this criterion indicates a possibly significant interphase temperature gradient, the magnitude of which can be estimated by[15]

$$\frac{\Delta T}{\Delta T^0} = \frac{Bi_m}{Bi_h} \cong 6\,5 \tag{8}$$

Table 2 Parametric values for the adiabatic reactor

Quantity	Value	Source
D_{eB}, D_{eT} (m^2/sec)	$4\ 5 \times 10^{-5}$	[4]
λ_e (J/m-sec-°C)	$5\ 1\lambda_{H_2} + 0\ 8\rho_g C_{p_g} U d_p$ (±10%)	[5]
$<\rho Cp>$ (J/m^3-°C)	$1\ 46\times10^{-6}$ (A4-A6) (±10%) $1\ 28\times10^{-6}$ (A7) $1\ 41\times10^{-6}$ (A8)	[5]
Cp_g (J/kmole-°C)	$(2\ 902x_H + 96\ 86x_B) \times 10^4$	[6]
MW_g (kg/kmole)	$2\ 106x_H + 78\ 12x_B$	-
ϵ	0 58 (±5%)	[5]
ρ_g (kg/m^3)	$C_B MW_g / x_B$	-
ρ_B (kg/m^3)	$4\ 14\times10^{-2}$ (A4) (±5%) $4\ 16\times10^{-2}$ (A5) $4\ 39\times10^{-2}$ (A6) $13\ 53\times10^{-2}$ (A7) $4\ 25\times10^{-2}$ (A8)	[5]
$(-\Delta H)$ (J/kmole)	$2\ 09\times10^8$	[7]
k^o (kmole/kg-sec-Pa)	$3\ 16\times10^{-2}$	[1]‡
K^o $(Pa)^{-1}$	$3\ 16\times10^{-13}$	[1]
E (J/kmole)	$5\ 76\times10^7$	[1]
Q (J/kmole)	$-6\ 89\times10^7$	[1]
k_d^o $(Pa\text{-}sec)^{-1}$	$1\ 80\times10^{-4}$	[1]
E_d (J/kmole)	$4\ 52\times10^6$	[1]
M_T (kg/kmole)	$4\ 05\times10^{-4}$ (A4) (±15%) $3\ 50\times10^{-4}$ (A5) (±5%) $4\ 14\times10^{-4}$ (A6) (±5%) $4\ 65\times10^{-4}$ (A7) (±2%) $5\ 11\times10^{-4}$ (A8) (±2%)	[5]

‡Individual estimates on the precision of kinetic parameters are not available, however Equation (5) with these values correlates observed hydrogenation rates to ±6% [8], Equation (4) correlates observed deactivation rates to ±15% [9]

Table 3 Catalyst effectiveness parameters

Quantity	Value	Source
Bi_h	≈ 1	[13]
Bi_m	≈ 6 5	assuming $j_d = j_h$
h (J/m^2-sec-°C)	≈ $2\ 2\times(10^2)$	
k_m (m/sec)	≈ $4\ 1\times(10^{-2})$	
r_B (kmole/m^3-sec)	≈ $k_1 C_B$ ≈ 0 162	assuming first order kinetics [2]
k_1 (m^3/kg-sec)	≈ $7\ 6\times(10^{-2})$	
ρ_c (kg/m^3)	$4\ 3\times(10^3)$	[16]
D_c (m^2/sec)	$5\ 2\times(10^{-6})$	[8]
λ_c (J/m-sec-°C)	0 15	[8]
Φ	$\Phi = r_p/3\sqrt{k_1\rho_c/D_c}$ = { 2 2 for 12 mesh; 1 1 for 20 mesh }	
γ	$\gamma = E/RT = 2700/1\ 98\ 413 = 3\ 3$	
β	$\beta = C_B^o(-\Delta H) D_c/\lambda_c T_B = 8\ 56\times(10^{-3})$	

That is, the interphase temperature gradient is several times that within the particle An overall effectiveness factor, reflecting the contributions of all gradients is given by[15]

$$\eta = \frac{3Bi_m}{\Phi^2}\left[\frac{\alpha - \tanh\alpha}{(Bi_m - 1)(\tanh\alpha + \alpha)}\right] \tag{9}$$

where

$$\Phi = \frac{r_p}{3}\sqrt{\left(\frac{k_1\rho_c}{D_c}\right)}$$

$$\alpha = \Phi \exp\left[\frac{\gamma}{2}(1 - 1/\theta')\right]$$

$$\theta' = 1 + \frac{\beta\eta}{3Bi_h}\Phi^2$$

Substitution of the parametric values from Table 3 in this expression gives $\eta \approx 0\,50$ for 12 mesh, $\eta \approx 0\,75$ for 20 mesh, and $\eta \approx 1\,0$ for 60 mesh particle sizes These values do not change appreciably with a two-fold increase in Biot number

Even though the net effectiveness is somewhat below unity in a number of runs, this has only a minor effect on the simulation At steady state and during poisoning the reaction zone, over which 100% conversion occurs, is very small ($\Delta z/L \leq 0\,05$) The net effect of the non-unity effectiveness factor is to increase the length of this zone by a small amount, in comparison with experimental profiles the difference is negligible and can be ignored This is so only because of the sharp reaction front, for less severe conditions, with the reaction zone extending throughout the bed, catalyst effectiveness would become a more important factor in modeling

Steady state simulation

Figure 4 demonstrates the generally good agreement of the steady state experimental results with the model These results may also be compared with those obtained from the analytical expression for the adiabatic temperature rise

$$(\Delta T)_{Ad} = \frac{(x_{B_0})(-\Delta H)}{(MW_g)(Cp_g)} \tag{10}$$

In Table 4 is given such a comparison among experimental observation, model calculations, and eqn (10) The three values are in good agreement with each other, the only trend noted is that model calculations are consistently about 5°C lower than experimentally observed values This is probably within the precision to be expected from the given set of experimental parameters, bed thermal conductivity is a particularly sensitive parameter, as will be discussed later

It can be seen in Fig 4 that all of the experimental profiles are shifted somewhat from the computed profiles, some as much as 6 mm Most of this discrepancy is due to annoying (and unexpected) difficulties in measuring the exact position of the catalyst bed in the reactor and of the thermocouple in the thermowell This shifting is not significant when comparing the dynamic profiles and is neglected in further discussion For Run A6, however, the large difference is apparently due to a gross error in measuring the location of the catalyst bed

Dynamic simulation

General comments Reported analyses of adiabatic fixed bed reactors in the absence of poisoning generally share two conclusions, (i) the thermal properties of the bed dominate the dynamic behavior, and (ii) the transient involves two distinct periods a fast concentration response (FCR)[17] where the temperature changes slowly but the concentration repidly achieves a quasi-steady state, and a slow temperature response (STR) where both temperature and concentration slowly evolve toward a final steady state

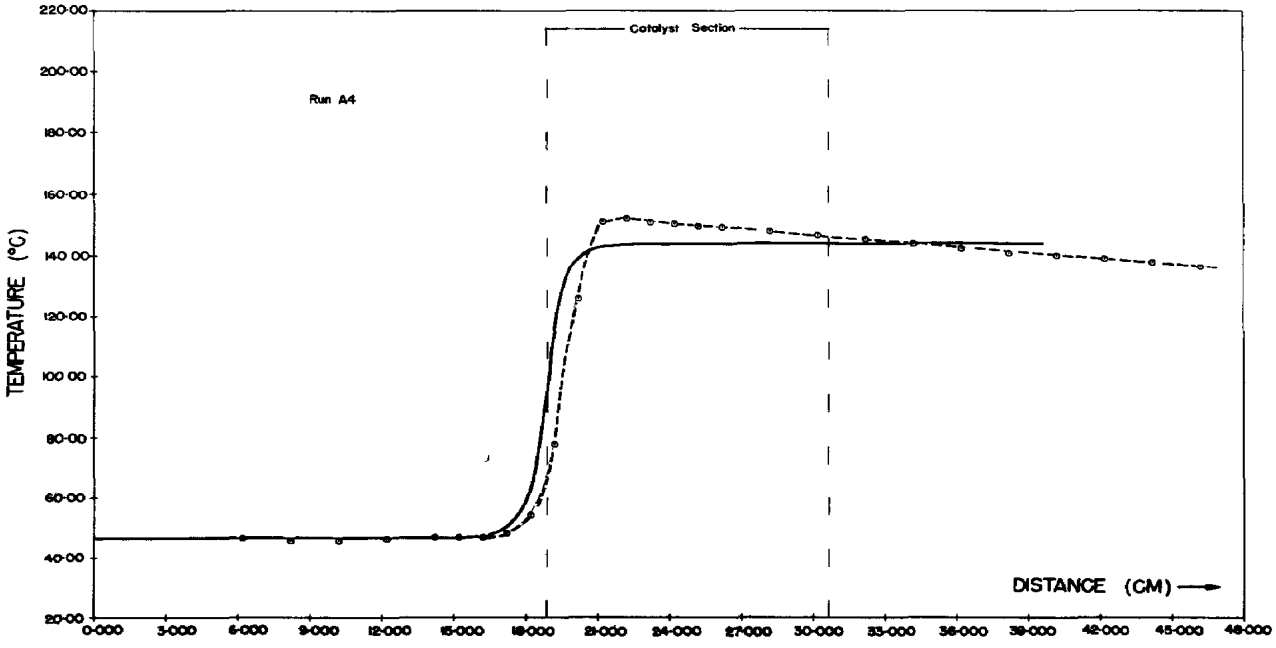

Fig 4 Results of steady state simulation for all runs ----, Experimental, ——, Computed

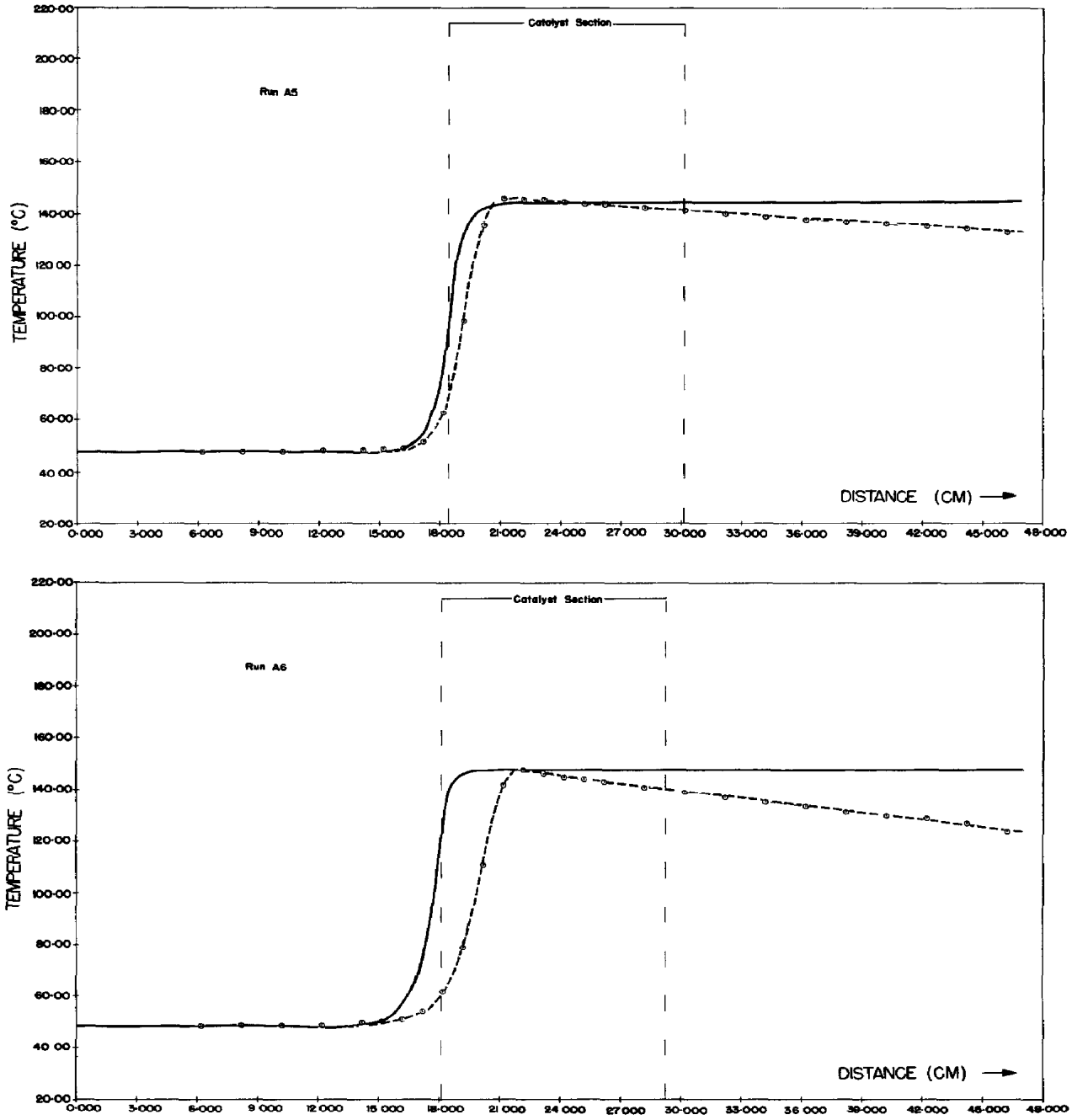

Fig 4 (*Cont*)

In the simulation of transients due to poisoning we find that the dynamics are composed of three, rather than two, distinct time domains, illustrated in Fig 5 for a typical calculation (conditions given in Table 1) The first domain is a FCR of thiophene, which very rapidly establishes a quasi steady profile from its zero initial condition This is not shown on the figure, since the profile is established within two residence times, during this period temperature, reactant and activity profile do not change significantly from their initial (steady state) values The other two domains can be classified as differing types of STR During the first of these (about 45 min in the example) the activity, reactant and poison concentration profiles slowly develop a characteristic shape which, during the second period, remain unchanged as the profile moves down the bed with constant velocity

A temperature maximum, in excess of the adiabatic temperature rise, is established in the first STR This additional temperature rise results from the convection of heat accumulated in the front of the bed while the initial steady state was achieved A similar phenomena has been noted in non-poisoned systems [18, 19] when the reaction zone is shifted downstream by a sudden perturbation in operating conditions

The second STR is the transient resulting from the poisoning of the catalyst Temperature, activity and

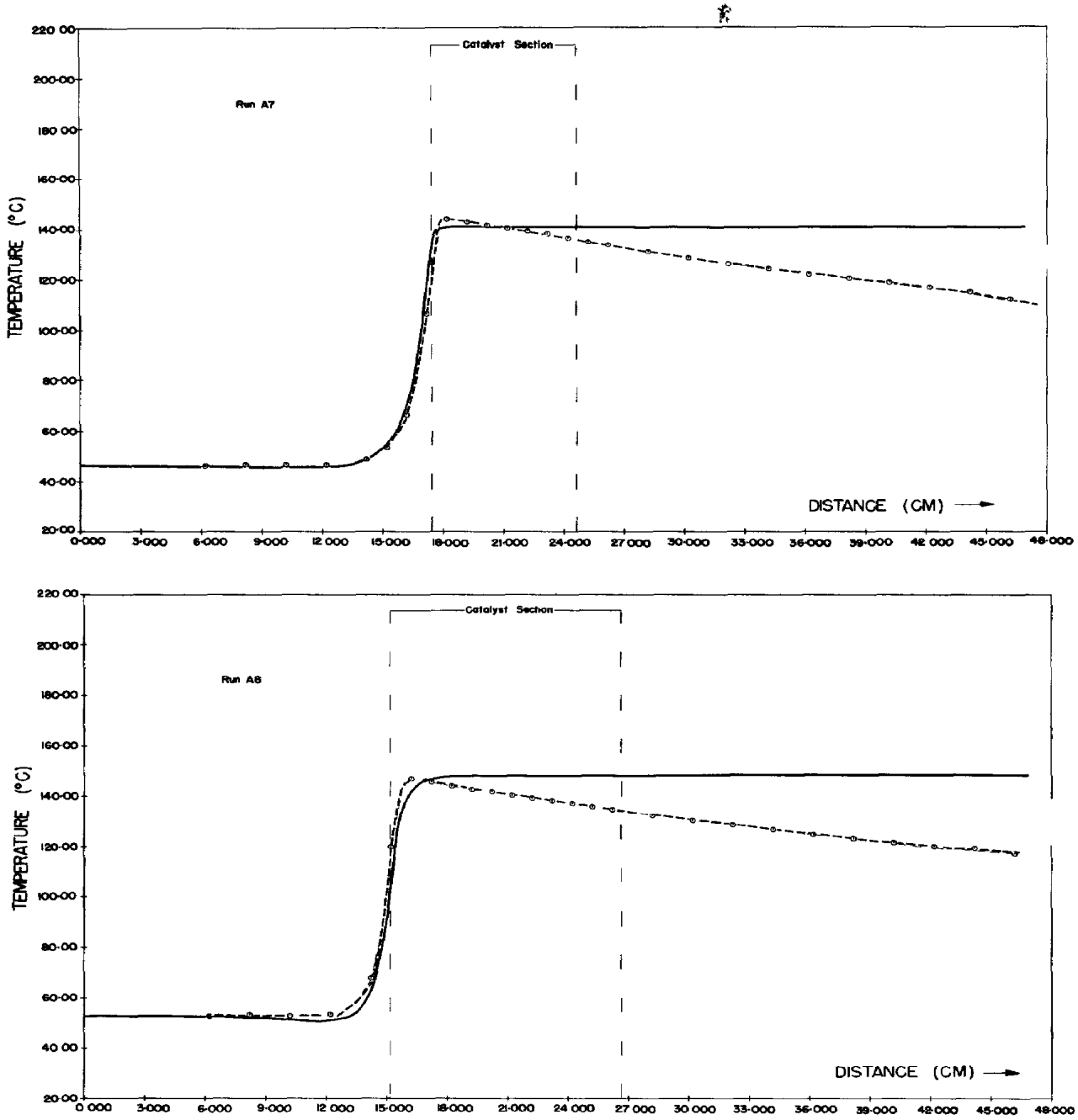

Fig 4 (*Cont*)

concentration profiles move through the bed without changing shape, the maximum temperature remains near the value established during the first STR

Dynamic simulation

Comparison with experiment It has been shown by Lyubarski *et al* [20] that the adsorption capacity of supported nickel for thiophene increases for temperatures in excess of 100°C due to a decomposition reaction which, under the conditions of the present experiments, is hydrogenolysis to *n*-butane The adsorption capacity was thus measured for each experiment, with the results given in Table 2 The larger experimental error associated with M_T for Run A4 reflects the difference between a spectrophotometric analysis used previously [9] and employed for this run, and the chromatographic method developed in this research used for subsequent runs

Comparison of the computed temperature profile transients with experimental data is given in Fig 6 for all runs In general the computed profiles are slightly steeper than experimental ones, and lag behind somewhat This behavior is probably the result of a combination of three factors (i) the temperature drops rapidly as the profiles exit the active section, which provides a very severe test of the precision of the hydrogenation and poisoning kinetics employed in the model, (ii) the rate of passage of the profiles through the bed is very sensitive to the value of M_T so that even relatively small experimental errors

Table 4 Comparison of adiabatic temperature rise values

Run	$(\Delta T)_{Ad}$ Equation (10)	$(\Delta T)_{Ad}$ Simulation	$(\Delta T)_{Ad}$ Experimental
A4	96 9°C	96 9°C	105 5°C
A5	97 6	96 7	98 1
A6	97 2	95 9	99 2
A7	99 4	95 0	98 0
A8	100 1	91 8	94 2

here become important, and (iii) shell progressive poisoning is occurring, as discussed later, so the bed, especially the latter part, appears to deactivate more rapidly than the uniform poisoning model predicts

Computed exit breakthrough curves for thiophene and benzene are shown in Fig 7 in comparison with the experimental data The agreement is again generally good in all cases, although the simulation is tardy in prediction of the point of incipient breakthrough for both substances This is to be expected on the basis of the behavior of the computed temperature profiles noted above Inspection of the shapes of the breakthrough curves on Fig 7 reveals that the actual concentration profiles in the bed are not as steep as those computed, further, the long tail on the thiophene breakthrough indicates that the bed is still capable of absorbing poison even when it is essentially inactive (i e benzene conversion less than one per cent) In most runs significant amounts of *n*-butane were detected in the reactor effluent, indicating that hydrogenolysis of thiophene was occurring and the deactivated catalytic surface was thus probably a nickel sulfide

Shell-progressive poisoning mechanism

If the adsorption capacity measures of Table 2 were intrinsic values, they should be approximately the same for all runs The differences shown lead to some conclusions regarding the mechanism of poisoning

The only significant difference between A6 and A7 is that the catalyst of A7 was exposed to poison twice as long, roughly 10% more poison was absorbed Runs A5 and A6 were carried out at different flow velocities and, if differences in the interphase mass transfer coefficients can be ignored, again the only significant difference is the exposure time Bed A6, exposed twice as long as A5, contained 20% more poison Bed A4 was exposed twice as long as A5 but to half the inlet thiophene concentration, similar M_T values indicate that these two conditions compensated one another Thus, comparison among A4, A5 and A6 indicates that doubling the inlet concentration leaves about 20% more poison in the catalyst for the same exposure time Finally, A5 and A8, at identical conditions except for particle size, demonstrate a 50% increase in capacity for the smaller particle size, where the external surface area per unit weight of catalyst was 450% higher

None of these differences is consistent with a uniform poisoning model, but they do conform to what might be expected qualitatively if the poisoning occurs by a shell-progressive mechanism The degree of deactivation in such a case will depend not only on operating conditions but also would be related to time of exposure in a non-linear manner The following simple analysis can be applied to the present results

By equating the rate of diffusion through the outer totally deactivated shell to the rate of reaction in the fully active inner core, one obtains[21]

$$\theta = \frac{1}{1/(1-\nu)+3\eta\Phi^2[1-(1-\nu)^{1/3}]/(1-\nu)^{1/3}} \qquad (11)$$

Where $\nu = M/M_T$, η = effectiveness factor for the inner core (~1 in our case), and Φ is the Thiele modulus for the entire pellet This result assumes first order kinetics, which is the case for benzene hydrogenation at the higher temperatures and low benzene concentrations of this study[2] Thus

$$-r_B = k_1 C_B \qquad (12)$$

where

$$k_1 = k^0 K^0 e^{-(Q+E)/RT} P^2 x_H \frac{MW_g}{\rho_g}$$

Inserting the appropriate parametric values for a temperature norm of 150°C gives $k_1 = 76\,2$ cm³/g-sec This in turn gives for the Thiele modulus

$$\Phi = \frac{r_p}{3}\left(\frac{k_1\rho_c}{D_c}\right)^{1/2} = 1\,9 \qquad (13)$$

Figure 8 compares the activity of this shell-progressive interpretation with a uniform poisoning model The severe non-linear relationship between activity and amount adsorbed for the larger particles indicates the existence of shell-progressive poisoning for runs with that catalyst

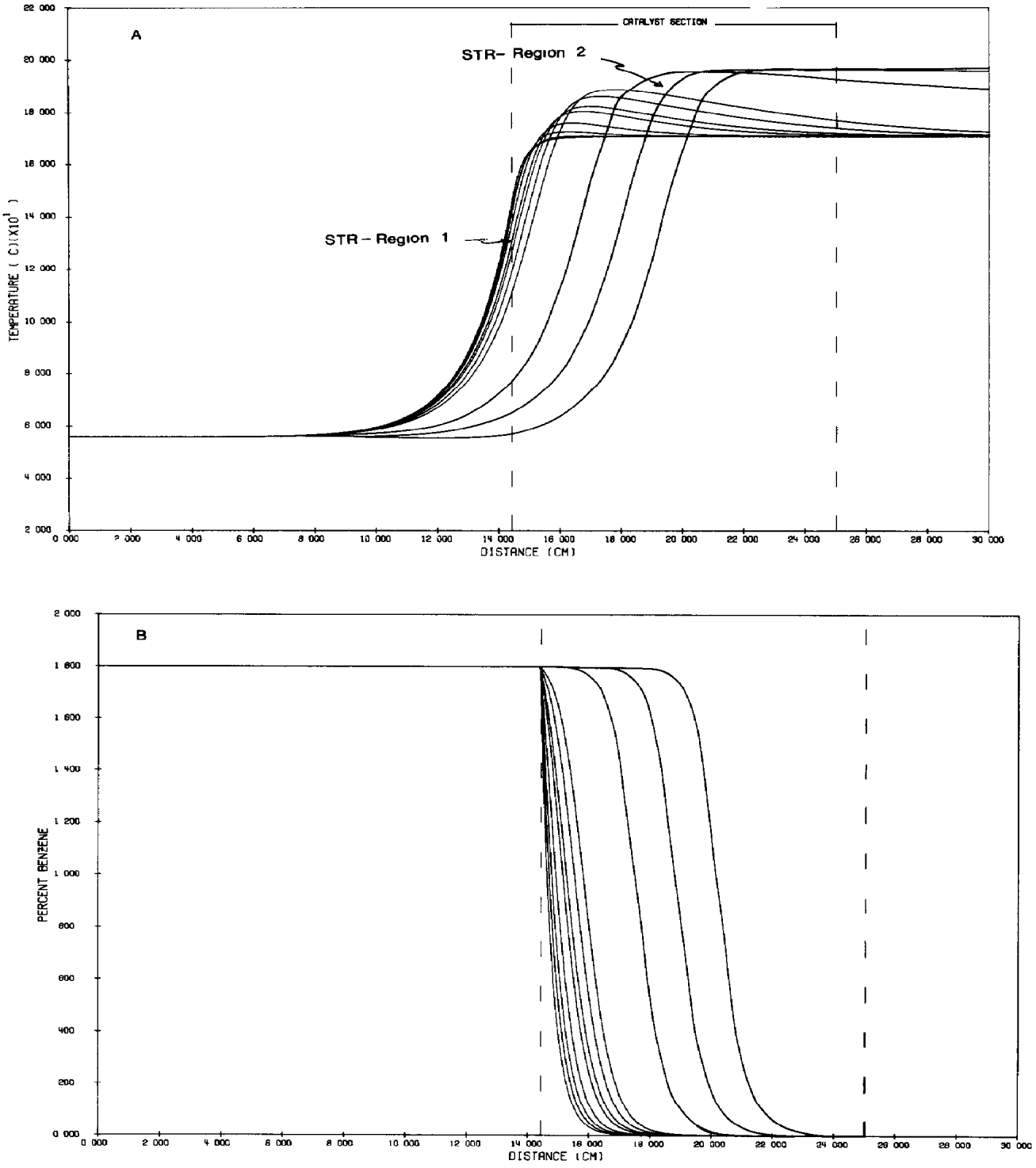

Fig 5 The general characteristics of dynamics induced by catalyst poisoning (a) Temperature response, (b) Bezene concentration response, (c) Catalyst activity response, (d) Thiophene concentration response Profiles plotted for STR Region 1 are 3 min apart, for STR Region 2 are 10 min apart Operating conditions as shown in Table 1

The analysis for the 60/70 mesh catalyst indicates near uniform poisoning (Run A8) and thus one would expect good agreement with the simulation for that case, this is indeed so Use of the individual M_T values for other runs in effect employs a lumped parameter incorporating the combined effects of poison adsorption capacity and the shell-progressive deactivation mechanism In such cases, the simulation based on uniform poisoning is adequate for the purpose of reactor modeling, but the parameter M_T is specific only to the conditions of the experiment

A completely different interpretation, based on a two site model for the poisoning of nickel by thiophene, was

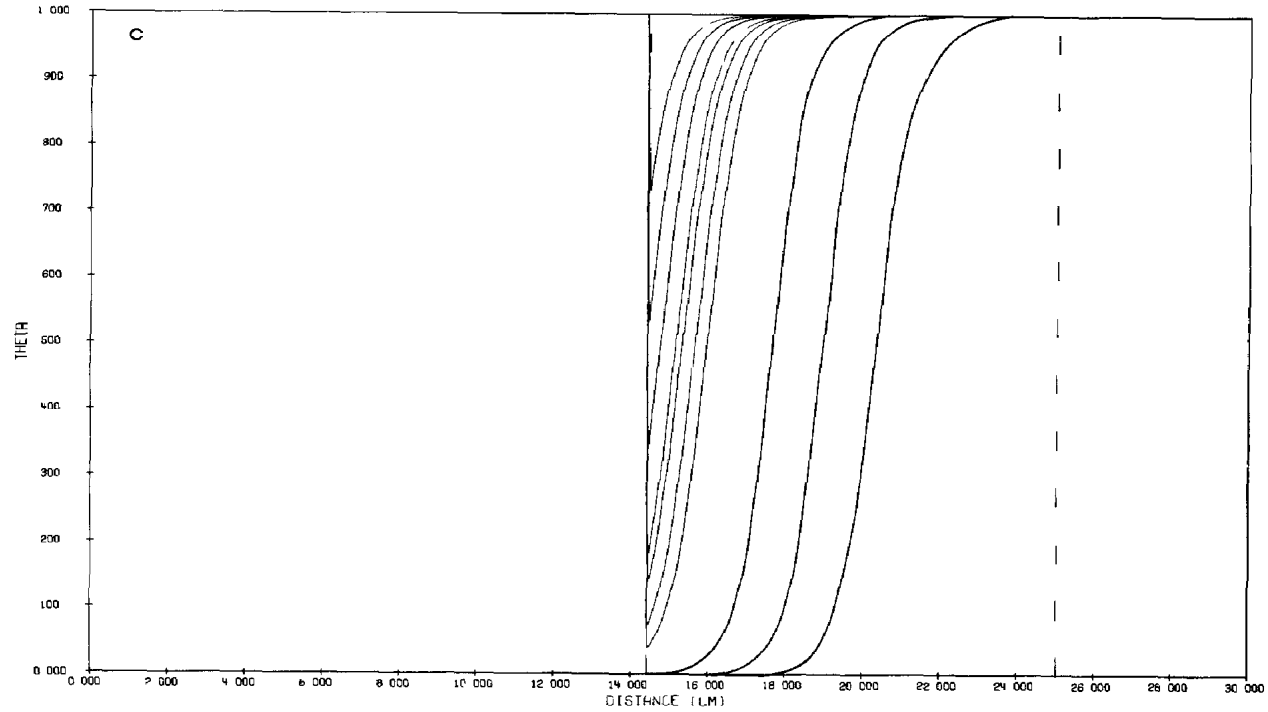

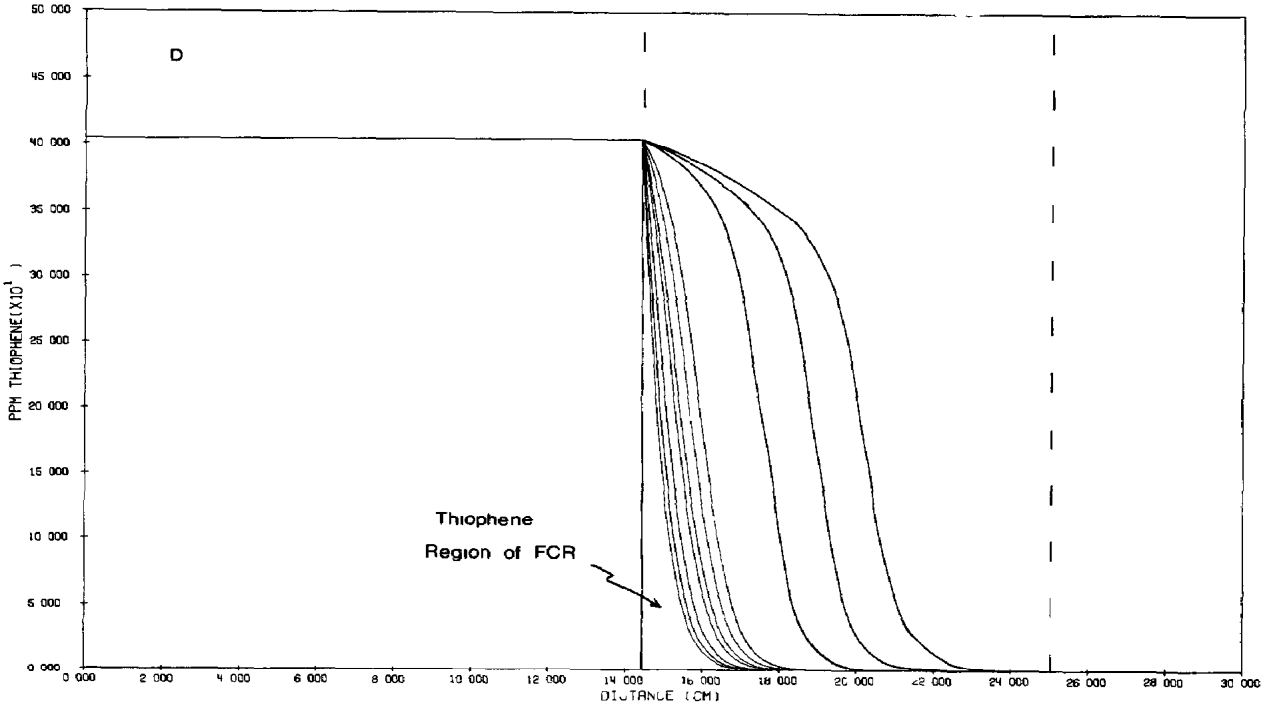

Fig 5. (*Cont*)

proposed in analysis of our previous results on non-adiabatic fixed bed dynamics[1] If data were available only for the 12/20 mesh catalyst, it would indeed be impossible to distinguish between the two interpretations Such results would then be a classical example of the question posed in the original discussion by Wheeler[22],

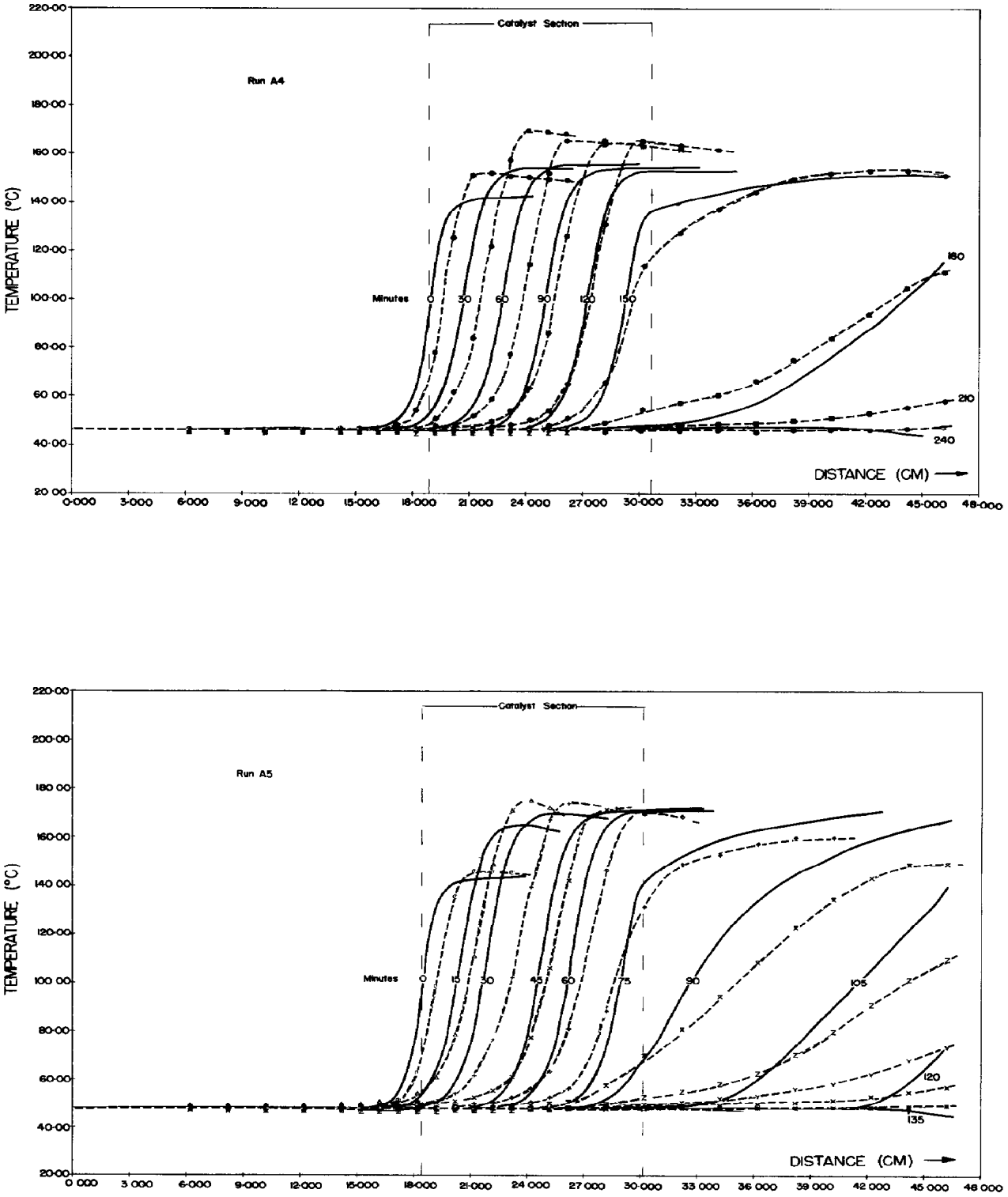

Fig 6 Results of the dynamic simulation of temperature profiles for all runs ----, Experimental, ——, Computed

i e are non-linear activity vs amount adsorbed correlations due to the intrinsic nature of bonding on the surface, or are they due to interactions between rates of diffusion, reaction and poisoning? In the present instance, the difference between 12/20 and 60/70 mesh provides one indication that shell-progressive deactivation is the proper interpretation Further supportive evidence is given in Fig 9 Here are plotted sulfur profiles, as measured with a scanning electon microprobe, within a large particle of Ni-kieselguhr catalyst poisoned under conditions of temperature and concentration identical to the fixed bed experiments[23] The sharp gradients shown are again

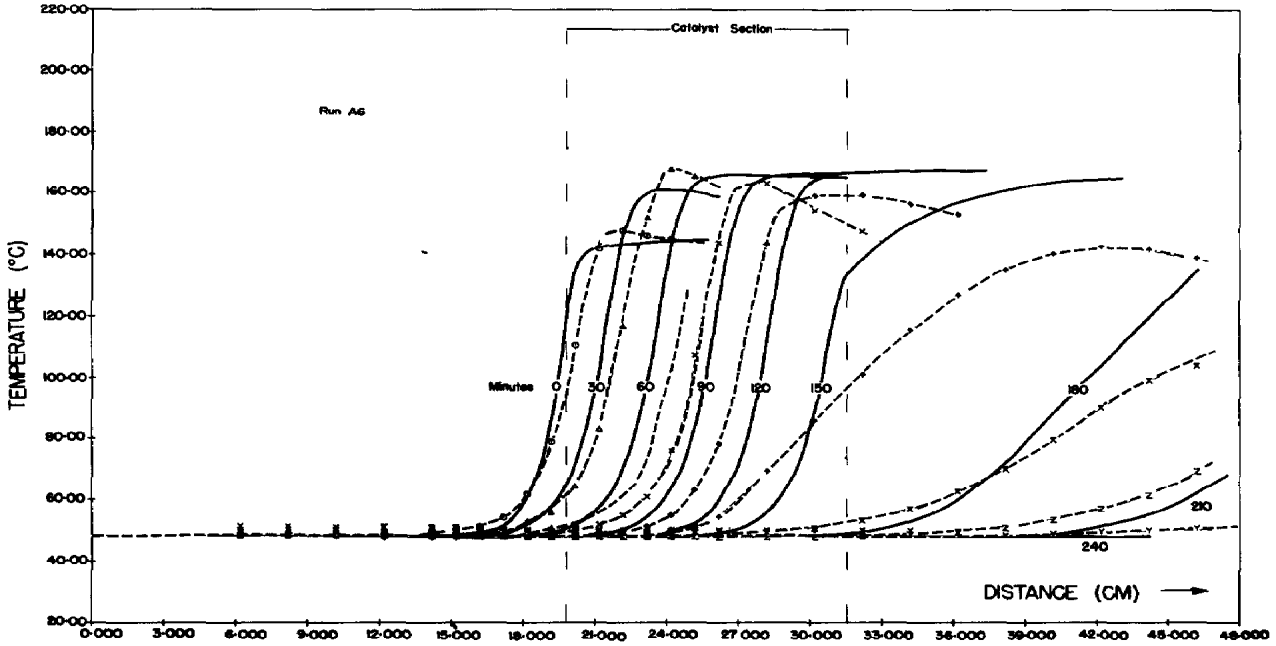

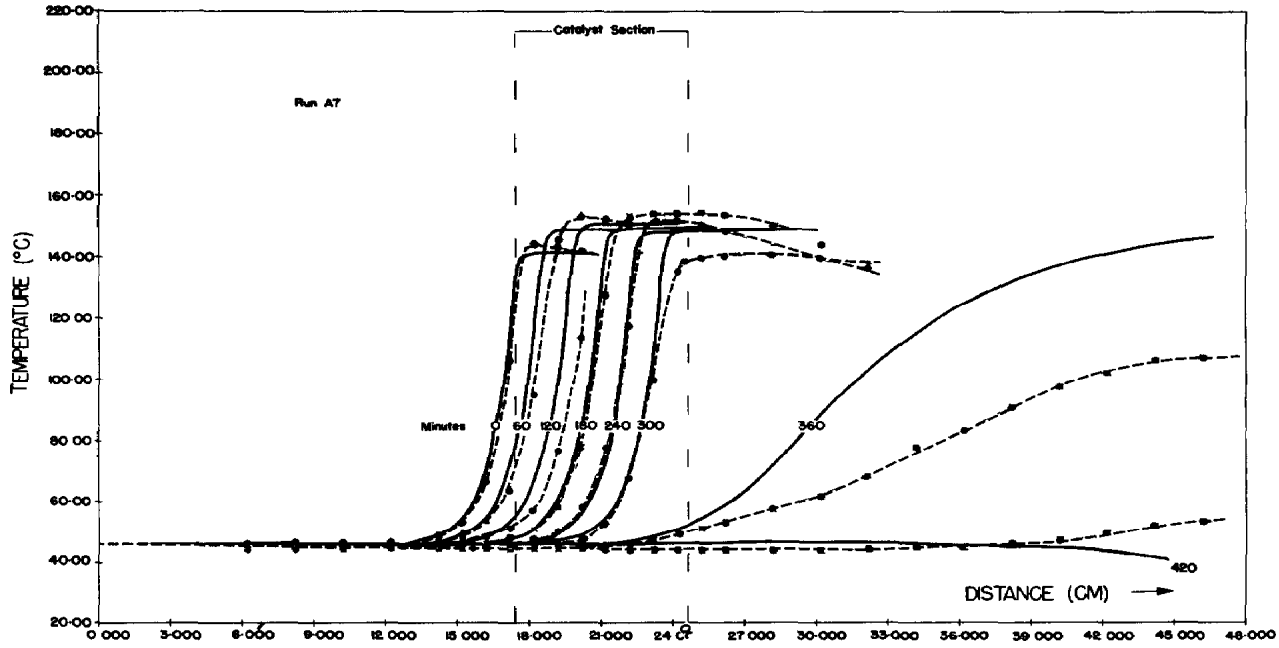

Fig 6 (*Cont*)

indication of a shell-progressive deactivation Although the effectiveness factor for this large pellet is smaller than for the 12/20 mesh catalyst ($\eta \sim 0\ 2$ vs $\sim 0\ 80$), we feel it is still possible to offer this as qualitative evidence supporting the shell-progressive mechanism

Dynamic temperature rise

It was mentioned earlier that during the first STR the reactor temperature maximum attains a value in excess of the adiabatic temperature rise established at steady state In Fig 10(a) the darkened area represents the effect of the

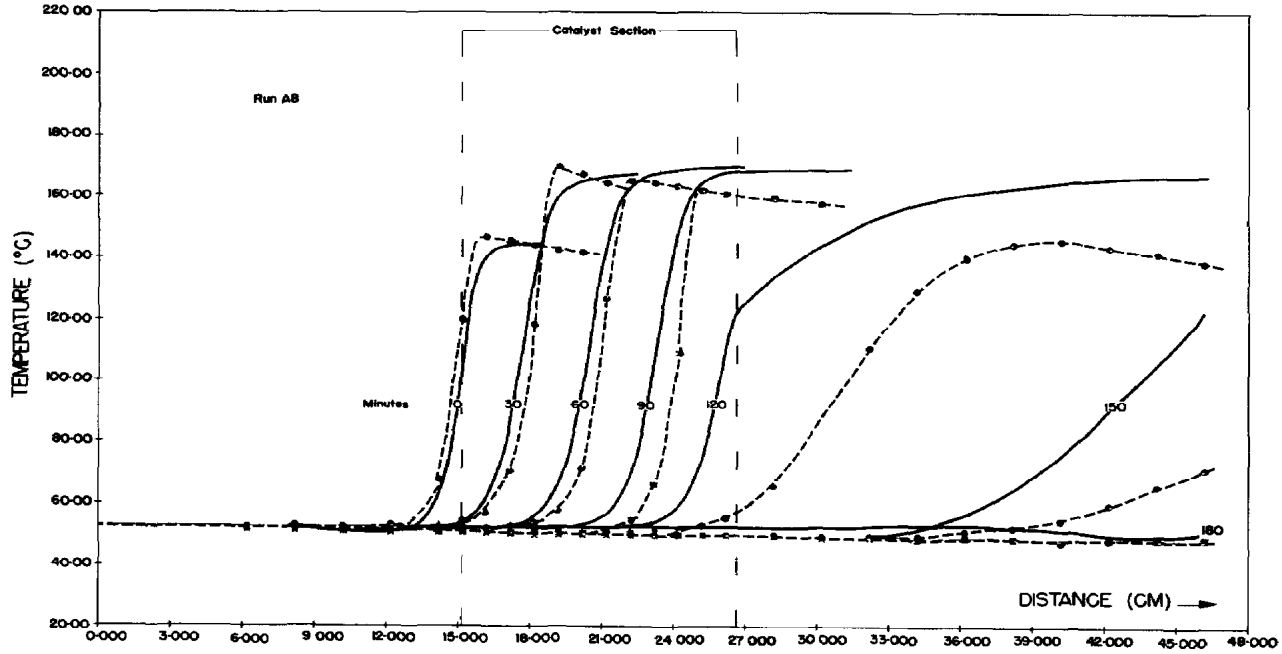

Fig 6 (*Cont*)

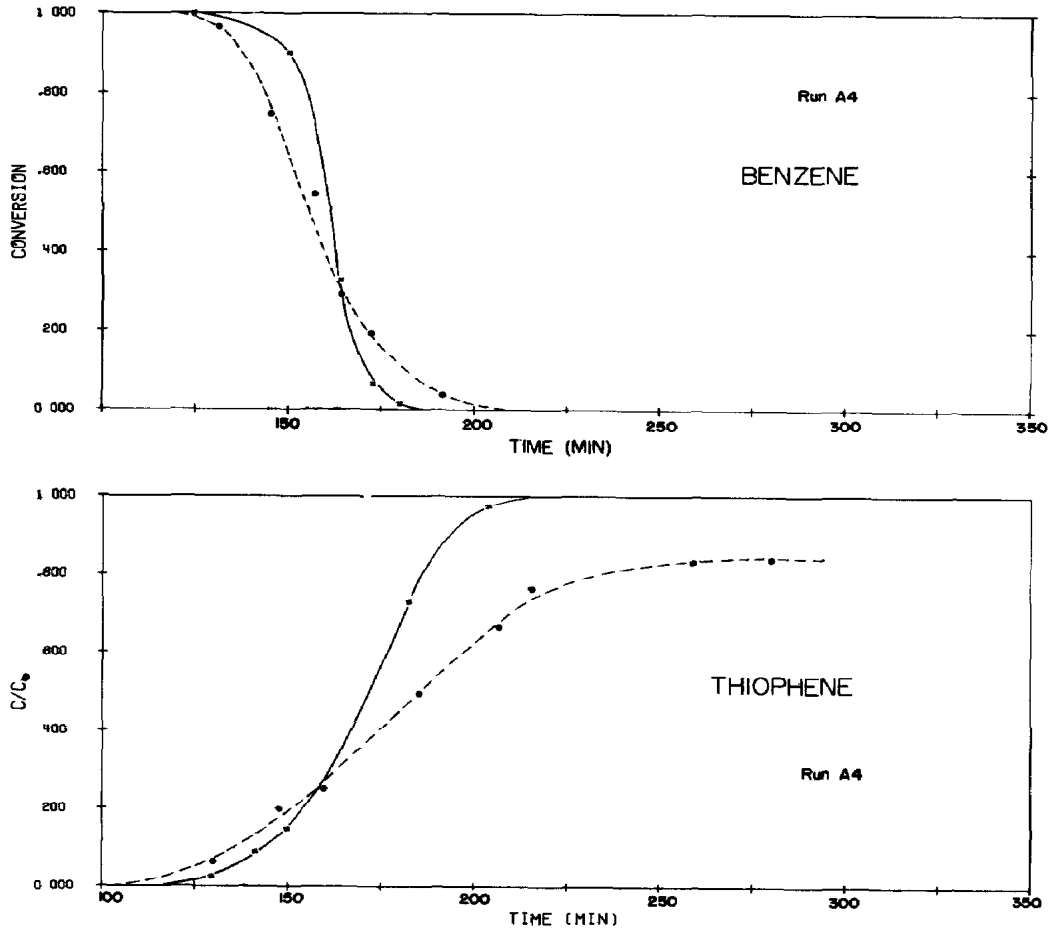

Fig 7 Results of the dynamic simulation of exit benzene and thiophene concentrations for all Runs ----, Experimental, ——, Computed

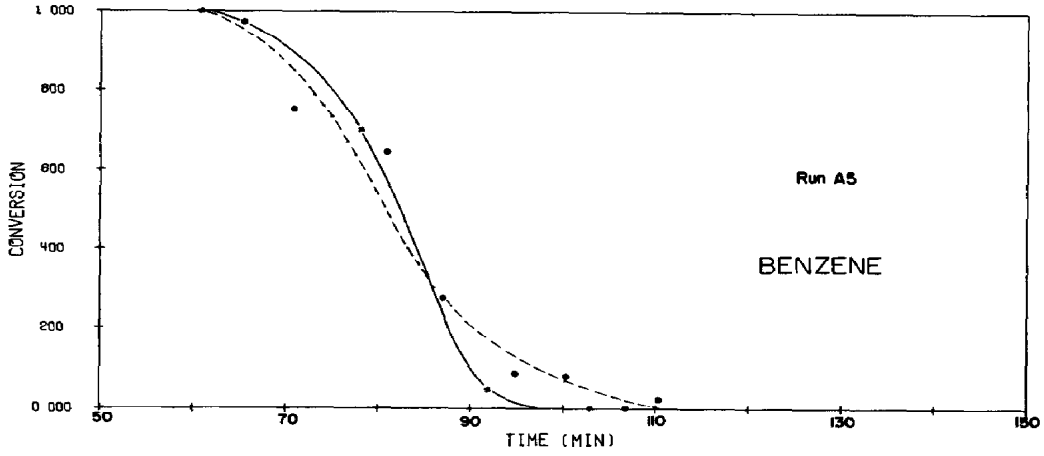
1 000
800
600
400
200
0 000
CONVERSION
Run A5
BENZENE
50
70
90
110
130
150
TIME (MIN)

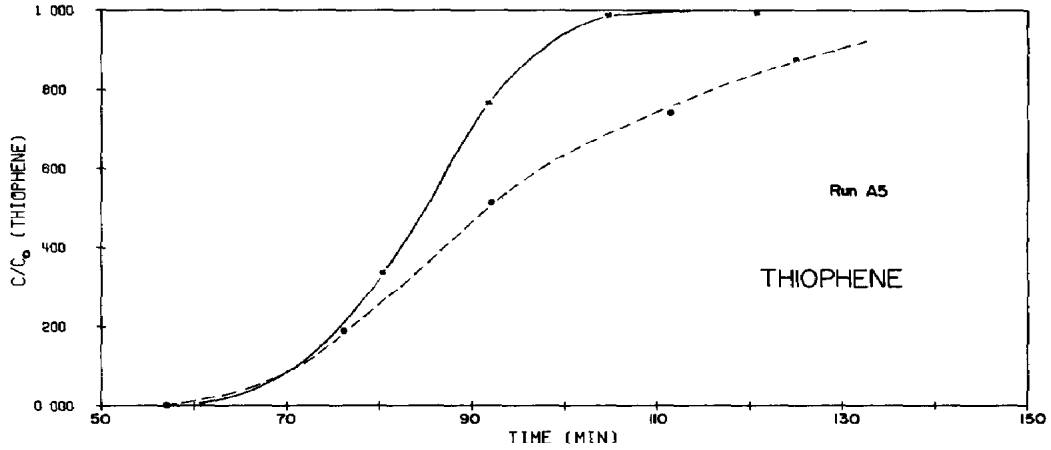
1 000
800
600
400
200
0 000
C/C0 (THIOPHENE)
Run A5
THIOPHENE
50
70
90
110
130
150
TIME (MIN)

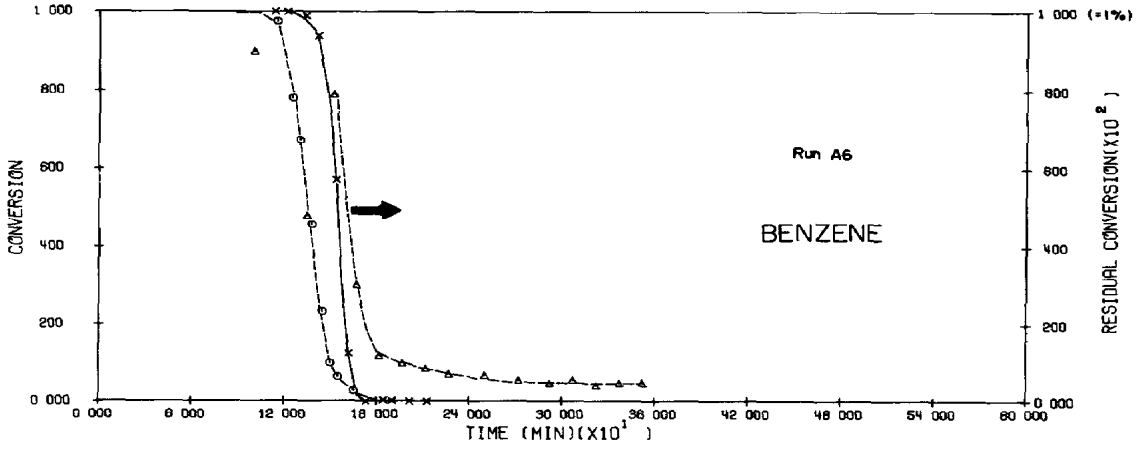
1 000
800
600
400
200
0 000
CONVERSION
Run A6
BENZENE
1 000 (=1%)
RESIDUAL CONVERSION(X10 2)
0 000
6 000
12 000
18 000
24 000
30 000
36 000
42 000
48 000
54 000
60 000
TIME (MIN)(X10 1)

Fig 7 (*Cont*)

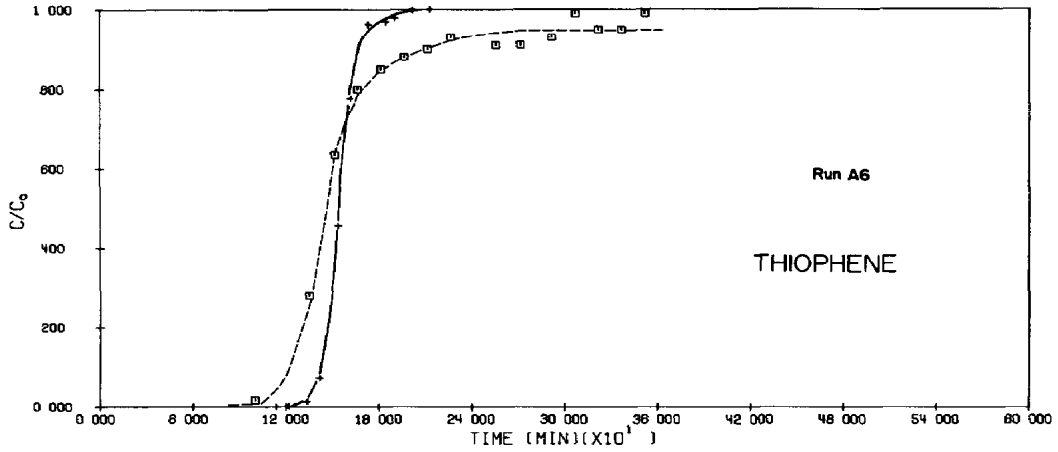
1 000
800
600
400
200
0 000
C/C0
Run A6
THIOPHENE
0 000
6 000
12 000
18 000
24 000
30 000
36 000
42 000
48 000
54 000
60 000
TIME (MIN)(X10¹)

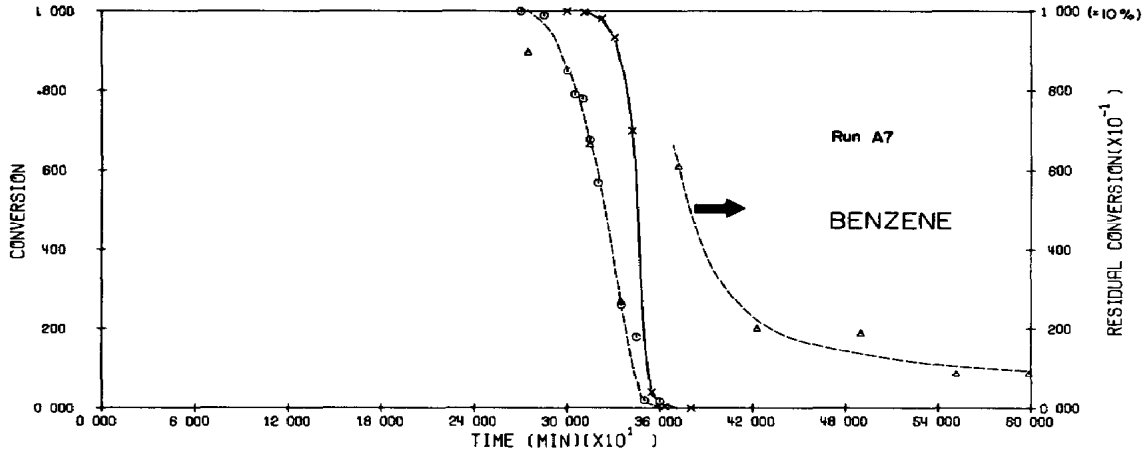
1 000
800
600
400
200
0 000
CONVERSION
1 000 (±10%)
800
600
400
200
0 000
RESIDUAL CONVERSION(X10⁻¹)
Run A7
BENZENE
0 000
6 000
12 000
18 000
24 000
30 000
36 000
42 000
48 000
54 000
60 000
TIME (MIN)(X10¹)

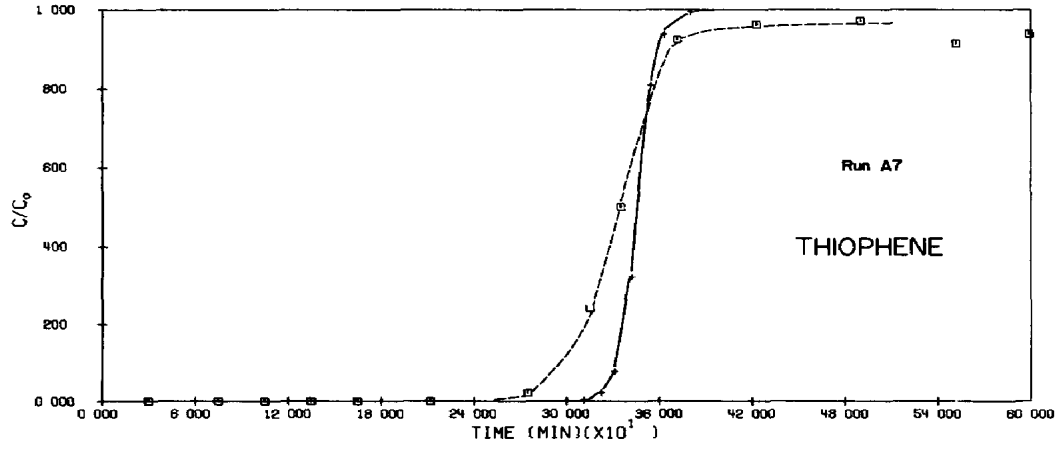
1 000
800
600
400
200
0 000
C/C0
Run A7
THIOPHENE
0 000
6 000
12 000
18 000
24 000
30 000
36 000
42 000
48 000
54 000
60 000
TIME (MIN)(X10¹)

Fig 7 (*Cont*)

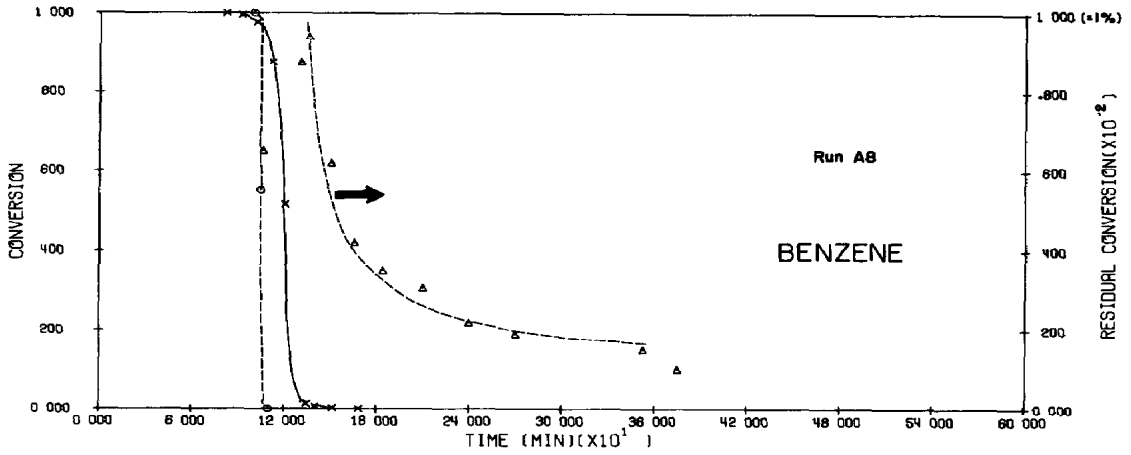

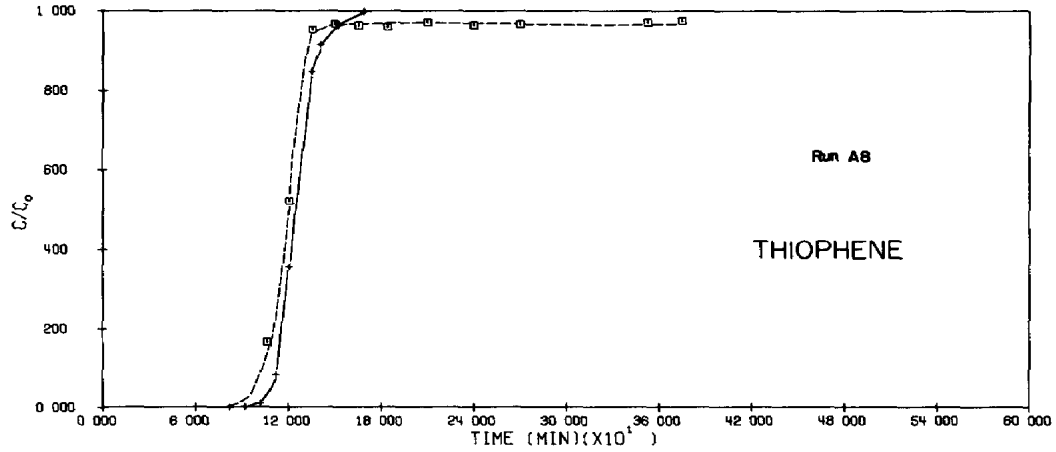

Fig 7 (*Cont*)

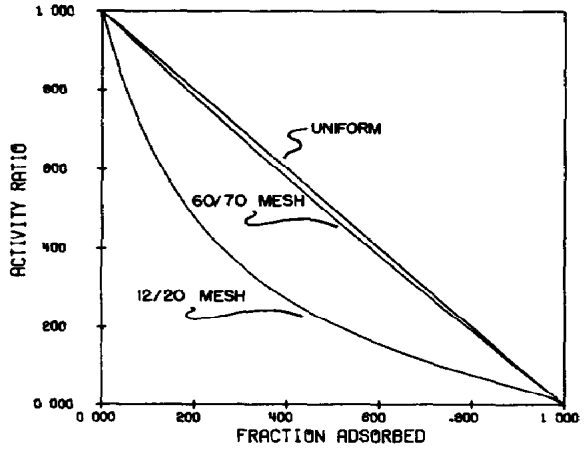

Fig 8 Relationship between activity and fraction adsorbed (ν) determined from eqn (11) for thiophene poisoning of benzene hydrogenation on Ni/Kieselguhr

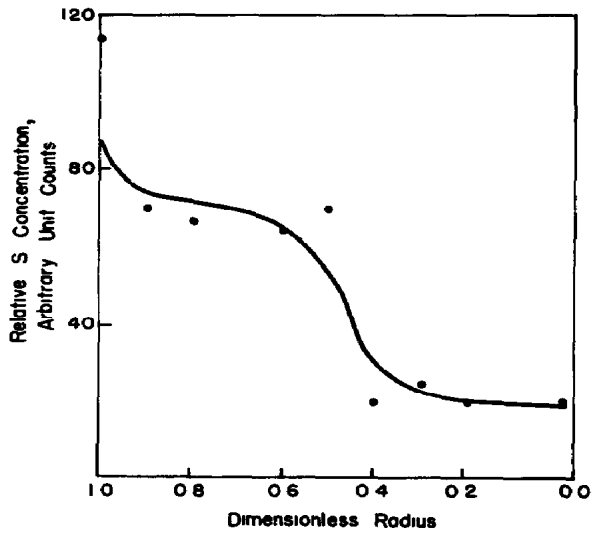

Fig 9 Typical sulfur profile within a deactivated catalyst particle as determined by a scanning electron microprobe

heat transferred from the solid between time t_0 and t_1 as the active zone moves down the bed This heat can only supplement that heat released in the reaction, and therefore must account for the increased temperature above $(\Delta T)_{Ad}$ Over the lifetime of the bed then the following simple balance should apply

(amount of heat accumulated at SS) =
(heat released during deactivation)

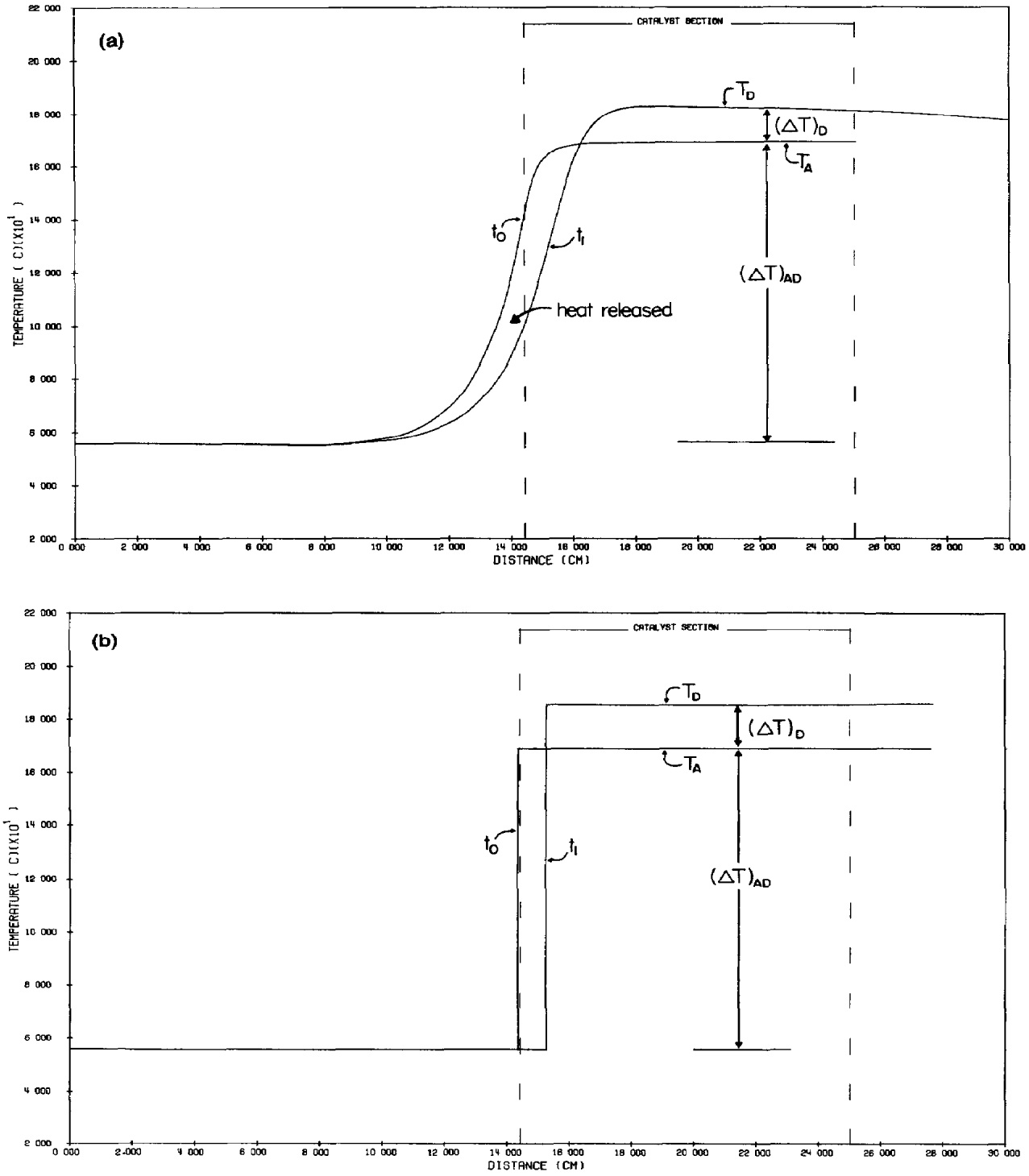

Fig 10 (a) Dynamic temperature rise and (b) its square wave approximation

or

$$\int_{Z1}^{Z2} [\langle \rho Cp \rangle (T - T_0)\, dz]_{ss} = \int_0^{t_s} [(\rho Cp)_g U (T - T_A)\, dt]_{poisoning} \quad (14)$$

Where $T_A = T_0 + (\Delta T)_{Ad}$ and t_s is the time required to fully deactivate the bed This is calculated from experimental parameters as

$$t_s = \frac{\rho_B M_T (Z2 - Z1)}{U C_T^0} \quad (15)$$

For adiabatic operation a good approximation is to assume that steady state and transient temperature profiles are square waves, as shown in Fig 10(b)

Equation (14) is then easily integrated to give, after substituting for t_s

$$(\overline{\Delta T})_D = \frac{C_T^0}{\rho_B M_T} \frac{\langle \rho Cp \rangle}{\langle \rho Cp \rangle_g} (\Delta T)_{Ad} \tag{16}$$

where $(\overline{\Delta T})_D$ is the dynamic temperature rise above $(\Delta T)_{Ad}$ The average velocity of the activity front is

$$U_p = \frac{C_T^0 U}{\rho_B M_T} \tag{17}$$

which gives finally for $(\overline{\Delta T})_D$

$$(\overline{\Delta T})_D = \left(\frac{U_p}{U}\right) \frac{\langle \rho Cp \rangle}{\langle \rho Cp \rangle_g} (\Delta T)_{Ad} \tag{18}$$

Several conclusions can now be drawn regarding this temperature rise it is (i) linear in all of the poisoning variables, (ii) dependent on inlet reactant concentration through $(\Delta T)_{Ad}$, (iii) has no indicated maximum value, and (iv) is independent of gas velocity through the bed (since U_p is proportional to U) This is only a time averaged value, from Fig 5 it is apparent that the temperature behaves somewhat differently for each STR domain

In Table 5 is given a comparison of the analysis detailed above with both experimental and computer simulation results The middle column of Table 5 shows that the simulation correctly predicts the effect of changes in C_T^0 (Runs A4 and A5), and the independence of $(\overline{\Delta T})_D$ from flow velocity (A5 and A6) Run A7 has about 3 times the catalyst density as A6, and the simulation gives about one-third the dynamic temperature rise Agreement between the simulation and experiment and the square wave analysis and experiment is generally good, with the exception of Run A8 where the estimated value is too low At present we have no explanation for this

Influence of thermal properties on reactor dynamics

Bed thermal conductivity and reactor inlet temperature were conditions not easily varied in these experiments, however, on the basis of the general agreement between simulation and experiment it was felt that model calculations could be used to explore the influence of these variables

Figure 11(a) shows, for the example conditions listed in Table 1, that an order of magnitude change in the bed thermal conductivity has a pronounced effect on the shape of the profile but only a minor influence on the magnitude and position of the temperature maximum In addition, the rate of movement of the profiles through the bed is not substantially affected by λ_e, though of course the profiles are spatially displaced from each other for the different values of this parameter

The effect of a 15°C increase in inlet temperature is shown in Fig 11(b) The temperature profiles, both steady state and dynamic, appear only to be shifted vertically by a corresponding amount and are not distorted One might expect this intuitively for an adiabatic steady state system, and the general nature of the dynamic profiles is inferred in eqn (18)

The dynamic temperature rise analysis also allows one to deduce something about the effect of $\langle \rho Cp \rangle$ on reactor dynamics As $\langle \rho Cp \rangle$ decreases, the maximum temperature must approach the adiabatic temperature rise, and this could become an important design variable in systems where the catalyst is susceptable to thermal damage Conversely, increasing $\langle \rho Cp \rangle$, in addition to increasing $(\overline{\Delta T})_D$, also increases the life of the first STR A very large value (say 5 times that of the illustration) could lead to a first STR which lasts longer than the life of the catalyst In such a case the development of invariant profiles, moving through the bed at constant velocity, would not occur and the general characteristics of the reactor dynamics would be quite different from those treated here

CONCLUSIONS

The interpretation of poisoning kinetics via a shell-progressive mechanism for this reaction system we feel provides a plausible alternative to the two site mechanism proposed previously, and is more in accord with the experimental observations on the variation of adsorption capacity with run conditions It is interesting that, in accord with prior investigators who have studied reactor dynamics under non-poisoning conditions, the transient behavior induced by poisoning is still more controlled by the thermal properties of the reactor than the thermochemical properties of the reaction A note of caution in this regard is advisable, however, since the activation energy for thiophene poisoning of nickel is very low and the entire deactivation process is correspondingly temperature insensitive

Examination of the assumptions involved in the pseudohomogeneous model used to simulate reactor dynamics has shown them to be reasonable for the conditions of this study One is then led to an interesting question Why, with apparently reasonable models for poisoning kinetics and reactor simulation and much effort devoted to independent determination of parameters, are we not able to do even better with the simulation? The

Table 5 Comparison of dynamic temperature rise values

Run	$(\Delta T)_D$ Equation (18)	$(\Delta T)_D$ Simulation	$(\Delta T)_D$ Experimental
A4	10 4	12 3	13 0
A5	20 8	26 3	24 2
A6	17 2	22 4	15 4
A7	7 0	9 7	10 2
A8	13 0	21 3	18 6

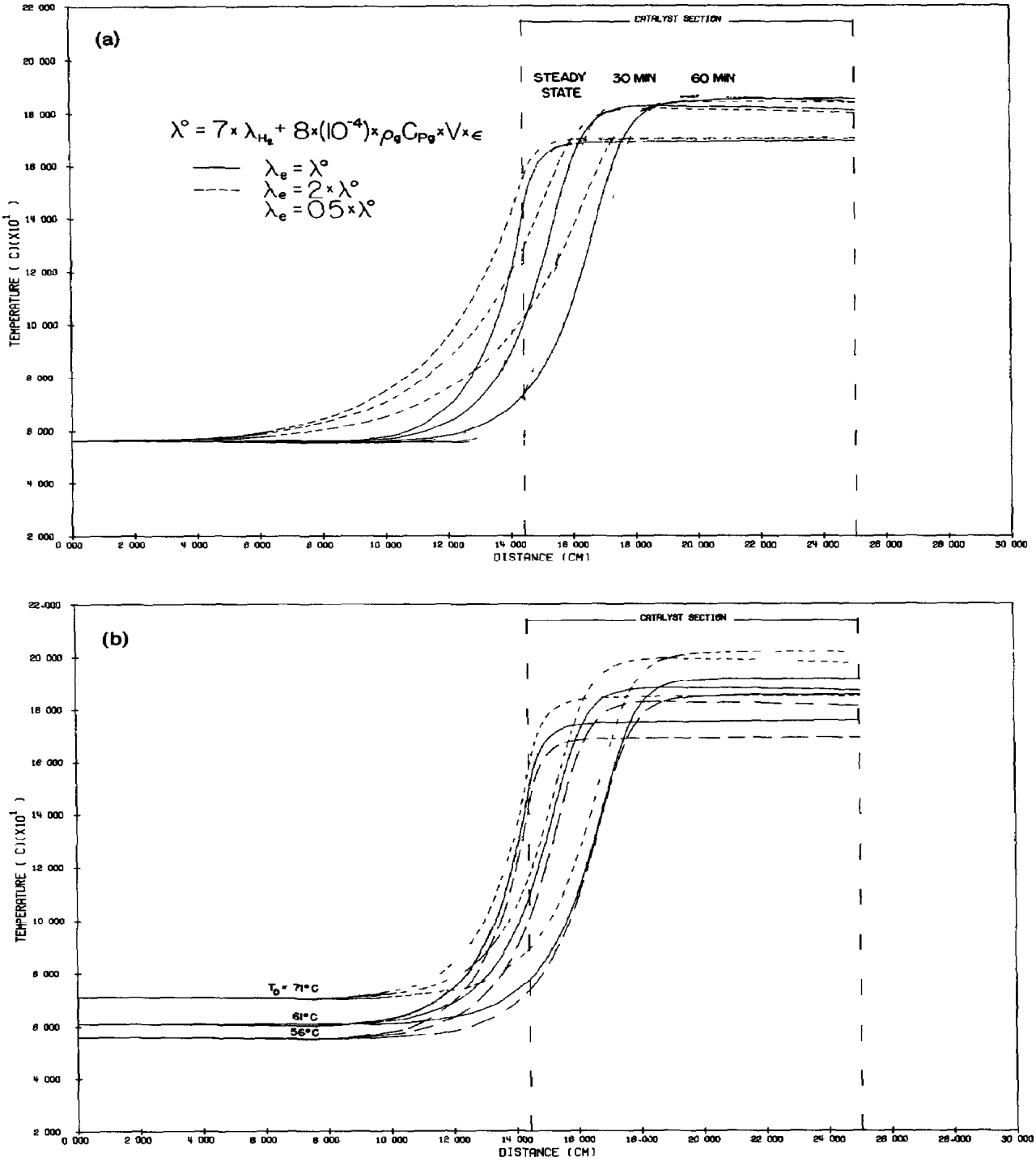

Fig 11 Influence of some thermal properties on the reactor dynamics (a) bed thermal conductivity and (b) feed temperature Conditions as shown in Table 1

problem of parametric sensitivity of such models is well known, and we see a good example of it here with respect to M_T However, quite aside from this there are clearly some pronounced effects on the simulation due to the accumulated uncertainties in the measured values of the parameters Three factors seem to be important in determining how well these reactor dynamics can be simulated

(1) Amplification of the accumulated errors associated with determination of individual parameters

(2) Changes in the parametric sensitivity of the model Modeling the unpoisoned bed or the initial stages of deactivation is not the same problem as modeling a reactor in the later stages of life

(3) Inadequacy of the pseudohomogeneous model Evaluation of the assumptions involved is based primarily on steady state considerations, the combination of transient conditions with large temperature gradients is sufficient to tax the capabilities of the most willing model

The picture which emerges on considering these factors

is somewhat a discouraging one The first factor, however, should be no surprise to those with experience in kinetic parameter estimation where, for a given precision in the model, the parameters should normally be determined to better than twice this value Changes in parametric sensitivity are also probably very important, not much appears to have been done in this area and a thorough study would be a formidable task, yet this seems to be no less than what the realities of this type of simulation required

Acknowledgements—This research was supported by the National Science Foundation under Grant GK-17200 and the Dow Chemical Co The authors are also indebted to G Eigenberger and V W Weekman, Jr for helpful discussion on how to make little reactors work like big ones

NOTATION

Bi_m Bi_h Biot numbers for mass and heat transfer, $Bi_m = (kmr_P/D_c)$, $Bi_h = (hr_p/\lambda_c)$
C_T^0 entrance concentration of thiophene, kmole/m³
C_B concentration of benzene, kmole/m³
Cp_g heat capacity of gas, J/kmole − °C
D_{eB}, D_{eT} dispersion coefficients for benzene and thiophene, m²/sec
D_c effective diffusivity of catalyst, m²/sec
E, E_D activation energies of hydrogenation and poisoning reactions, J/kmole
$(-\Delta H)$ heat of reaction, J/kmole
h heat transfer coefficient, J/m² − sec − °C
k_1 first order rate constant for hydrogenation reaction, m³/kmole − sec
k^0 pre-exponential factor for hydrogenation reaction, kmole/kg − sec − N/m²
K^0 adsorption constant for benzene, $(N/m^2)^{-1}$
k_d^0 pre-exponential factor for poisoning, $[(N/m^2) - sec]^{-1}$
km mass transfer coefficient, m/sec
L reactor length, m
MW_g molecular weight of gas, kg/mole
M_T poison adsorption capacity of catalyst, kg/mole
P pressure, N/m²
Pe_m, Pe_h Peclet numbers for mass and heat dispersion, $Pe_m = (2Ur_p/D_e)$, $Pe_h = (2\rho_g Cp_g Ur_p/\lambda_e)$
Q benzene adsorption activation energy, J/kmole
R gas constant, J/kmole − °C
r_p catalyst particle radius, m
r_B, r_T rates of benzene hydrogenation and thiophene chemisorption, kmole/kg − sec
r_d rate of activity decay, $(sec)^{-1}$
t time, sec
t_s time for complete deactivation of bed, sec
T bulk gas temperature, °C
T_A adiabatic maximum temperature, °C
ΔT interphase temperature difference, °C
ΔT^0 intraphase temperature difference, °C
$(\Delta T)_{Ad}$ adiabatic temperature rise, °C
$(\Delta T)_D$ dynamic temperature rise, °C
U interstitial velocity, m/sec
x_B, x_T, x_H mole fractions of benzene, thiophene and hydrogen
x_{B0} inlet mole fraction of benzene
z axial distance coordinate, m
$Z1$, $Z2$ location of catalyst bed entrance and exit, respectively, m

Greek symbols

α parameter of eqn (9)
β heat generation parameter, Table 3
γ activation energy parameter, Table 3
ϵ bed void fraction
η catalyst effectiveness factor
θ catalyst relative activity
λ_e, λ_c effective thermal conductivity of bed and catalyst, respectively, J/m − sec − °C
ν relative poison uptake on catalyst, eqn (11)
ρ_B bulk catalyst density, kg/m³
ρ_c, ρ_g catalyst particle and gas densities, respectively, kg/m³
$\langle \rho Cp \rangle$ effective heat capacity, of reactor, J/m³ − °C
Φ Thiele modulus
Φ' parameter of eqn (9)

REFERENCES

[1] Weng H-S , Eigenberger G and Butt J B , *Chem Engng Sci* 1975 **30** 1281
[2] Kehoe J P G and Butt J B , *J Appl Chem Biotechnol* 1972 **23** 22
[3] Szepe S and Levenspiel O , *4th European Symp on Chem Reaction Engng* p 265 Pergamon Press, Oxford 1970
[4] Krischer O and Kroll K , *Die Wissenschaftlichen Grundlagen der Trockangstechnik*, p 176 Springer-Verlag, Berlin 1963
[5] Price T H , M S Thesis, Northwestern University, Evanston, IL 1975
[6] Am Pet Institute, *Project 44 Tables* Carnegie Press, Pittsburgh 1953
[7] Conent J B and Kistiakowski G B , *Chem Rev* 1937 **20**, 181
[8] Kehoe J P G , Ph D Dissertation, Yale University, New Haven, CT 1971
[9] Weng H-S , Ph D Dissertation, Northwestern University, Evanston, IL 1974 Available from University Microfilms
[10] Evans E V and Kenney C N , *Trans Instn Chem Engr* 1966 **44** T189
[11] Yagi S and Kunii D , *A I Ch E J* 1957 **3** 373
[12] Butt J B and Weekman V W Jr , *A I Ch E Symp Ser* 1975 **70(143)** 27
[13] Littman H , Barile R G and Pulsifer A H , *Ind Engng Chem Fundl* 1968 **7** 554
[14] Mears D E , *J Catal* 1971 **20** 127
[15] McGreavy C and Cresswell D L , *Can J Chem Engr* 1969 **47** 583
[16] Data supplied by Harshaw
[17] Doesburg H V and DeJong W A , *Adv Chem* 1974 **133** 37
[18] Eigenberger G , *Adv Chem* **133** 36 (1974)
[19] Hansen K W , *Chem Engng Sci* **28**, 723 (1973)
[20] Lyubarski G D , Andeeva L B and Kul'Kova N V , *Kin i Kat* 1962 **3** 123 1963 **1** 382
[21] Smith J M , *Chemical Engineering Kinetics*, 2nd Edn McGraw-Hill, New York 1970
[22] Wheeler A , *Catalysis* (Edited by Emmett P H), Vol II Reinhold, New York 1955
[23] Lee J W , Ph D Dissertation, Northwestern University, Evanston, IL 1975 Available from University Microfilms